

# THE ASTROPHYSICAL JOURNAL

VOLUME 141

APRIL 1, 1965

NUMBER 3

## EXPLORER XI EXPERIMENT ON COSMIC GAMMA RAYS\*

W. KRAUSHAAR, G. W. CLARK, G. GARMIRE, H. HELMKEN,†  
P. HIGBIE, AND M. AGOGINO‡

Department of Physics and Laboratory for Nuclear Science,  
Massachusetts Institute of Technology, Cambridge, Massachusetts

*Received November 23, 1964*

### ABSTRACT

A search for cosmic gamma rays in the energy range 100 MeV and greater with the satellite Explorer XI has given an apparent average intensity of about  $3 \times 10^{-4} \text{ cm}^{-2} \text{ sec}^{-1} \text{ sterad}^{-1}$ . Internal evidence favors the identification of the particles which give rise to this intensity as cosmic gamma rays, but because a celestial anisotropy is not evident the measurement must be regarded as an upper limit on the true intensity. The apparent intensity is 10 to 20 times as large as predicted for  $\pi^0$ -decay gamma rays from cosmic-ray collisions with interstellar hydrogen, but can be accounted for if one assumes a modest intensity of high-energy electrons in intergalactic space.

### I. INTRODUCTION

The intensity and distribution of arrival directions of cosmic gamma rays have important bearing on a number of problems of astrophysical interest. The most important mechanisms by which cosmic gamma rays in the region over 50 MeV can be produced are probably (*a*) collisions of cosmic-ray particles with gas and the production of  $\pi^0$  mesons which decay into gamma rays; (*b*) collisions of cosmic-ray electrons with the optical photons of starlight and the resulting production of high-energy "inverse Compton" gamma rays; and (*c*) collisions of cosmic-ray electrons with gas and the production of bremsstrahlung gamma rays. Our estimates indicate that, for interstellar space, mechanism (*a*) is the most important, and that, as pointed out by Felten and Morrison (1963), mechanism (*b*) may be important if appreciable numbers of energetic electrons exist in intergalactic space. Mechanism (*a*) could be of significance in intergalactic space if the cosmic-ray intensity there is comparable to its local value and if the gas density is comparable to the cosmological value,  $10^{-5}$  protons  $\text{cm}^{-3}$ .

Estimates of the intensity of gamma rays produced by the above mechanisms have been made by a number of authors (Morrison 1958; Savedoff 1959; Greisen 1960; Kraushaar and Clark 1962; Pollack and Fazio 1963). The estimates depend, of course, upon what is assumed for the various astrophysical quantities. For example, if it is

\* This work has been supported in part by the National Aeronautics and Space Administration under Contract NASw37 and Grant NsG-386 and in part by the U.S. Atomic Energy Commission under Contract AT(30-1)2098.

† Now at Smithsonian Astrophysical Observatory, Cambridge, Massachusetts.

‡ Now at Eastern New Mexico University, Potosi, New Mexico.

assumed that the cosmic-ray flux throughout our Galaxy is about the same as it is near the Earth and that the only interstellar gas is the atomic hydrogen as measured by the radio astronomical 21-cm observations, then the gamma-ray intensity averaged over all directions is predicted to be of the order of  $10^{-5} \text{ cm}^{-2} \text{ sec}^{-1} \text{ sterad}^{-1}$ . This is some 4 orders of magnitude smaller than the charged-particle cosmic-ray intensity to which any detector is necessarily subject and places severe demands upon the detector and its ability to reject possible sources of background.

The preliminary results of the Explorer XI satellite experiment, which was designed as an exploratory experiment to detect these gamma rays, have already been published (Kraushaar and Clark 1962). Our data at the time of these reports were scanty, but, because the events we had detected showed some of the expected tendency to cluster about the galactic center and galactic plane, we were encouraged. All the data have now been analyzed. There remains no statistically convincing evidence for celestial anisotropy. All the internal tests at our disposal are consistent with the apparent intensity we have measured being the true intensity of cosmic gamma rays and not background, but lacking the evidence of a celestial anisotropy, only an upper-limit measurement can be claimed.

## II. THE INSTRUMENT

The gamma-ray detector was mounted within an aluminum housing. The outside of this housing carried the solar cells which provided the battery-charging power. The fourth-stage solid-fuel rocket motor remained attached to the instrument in orbit. The complete satellite is shown in Figure 1, and a schematic drawing of the detector is shown in Figure 2.

The arrival of a gamma ray was signaled by a coincidence between the sandwich scintillation counter and the Cerenkov counter, provided no pulse was received from the large cone-shaped anticoincidence or veto plastic scintillation counter. The sandwich counter, which consisted of five alternate slabs of cesium iodide and sodium iodide, served as a gamma-ray converter as well as one of the elements of the charged-particle telescope which defined the nominal solid angle of the detector. Immediately after the logic circuits sensed an event as defined above, information concerning the charged-particle energy loss in the sodium iodide and in the cesium iodide was telemetered. This feature was intended to provide data of help in identifying certain sorts of background, particularly that arising from neutron interactions in the sandwich detector. Unfortunately, one portion of the telemetry system failed shortly after launch and we were left with only one of the two pulse-height data channels. Fortunately, the data we had were sufficient to eliminate neutron interactions as a likely source of background.

The veto counter was disconnected by radio command for one orbit every day or so to permit the recording of incident charged particles and so provide a rough check on the detector operation. In addition, there was a twelve-stage binary scaler with telemetered outputs at scales of 64 and 4096. The input to this scaler was cycled among the various counting circuits (5 in all) also by radio command and provided reassuring checks as well as useful data on the radiation belts (Garmire 1963).

The solid-angle-area factor of the telescope was about  $4.3 \text{ cm}^2 \text{ sterad}$  and was determined from the geometry and sea-level counting rate of mu mesons. The efficiency of the instrument as a gamma-ray detector was measured as a function of gamma-ray energy first at the M.I.T. synchrotron using photo-produced  $\pi^0$ -decay gamma rays, and then later at the California Institute of Technology using a tagged gamma-ray beam.<sup>1</sup>

<sup>1</sup> A magnetically selected nearly monoenergetic beam of secondary electrons struck a thin aluminum target. A beam of gamma rays proceeded from this target through a 3-inch hole in a lead wall behind which was located either the detector or a large lead-glass Cerenkov counter. The electrons were reanalyzed by a second magnet and a small momentum interval selected by a counter placed in coincidence with two defining counters in the monoenergetic electron beam. A threefold coincidence thus indicated that a gamma ray of known energy was headed in the direction of the detector. The hole in the lead wall was somewhat larger than the sandwich detector in the gamma-ray detector but smaller than the lead-

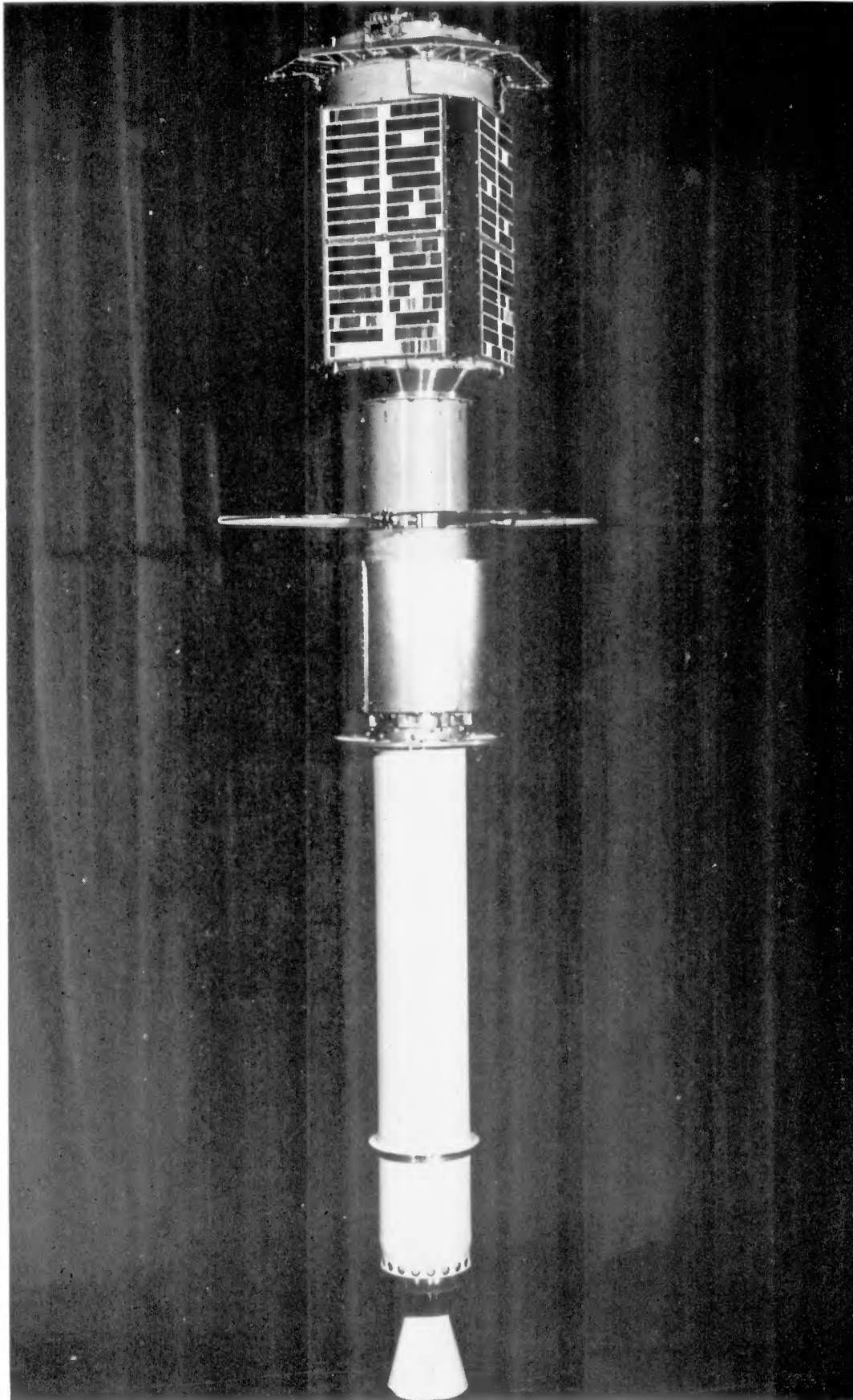


FIG. 1.—The complete Explorer XI satellite. The rocket motor remained attached and the elongated body tumbled about a transverse axis in a plane which slowly precessed.

The results of these efficiency measurements have been expressed in terms of equivalent detector area and are shown as a function of gamma-ray energy for forward incidence in Figure 3 and as a function of angle of incidence for 105 and 405 MeV in Figure 4. The actual area of the sandwich detector was 45 cm<sup>2</sup>, so that the detector efficiency for high energies was about 15 per cent in the forward direction.

The energy spectrum of gamma rays produced high in the Earth's atmosphere by cosmic rays has been measured by Carlson, Hooper, and King (1950) and by Svensson

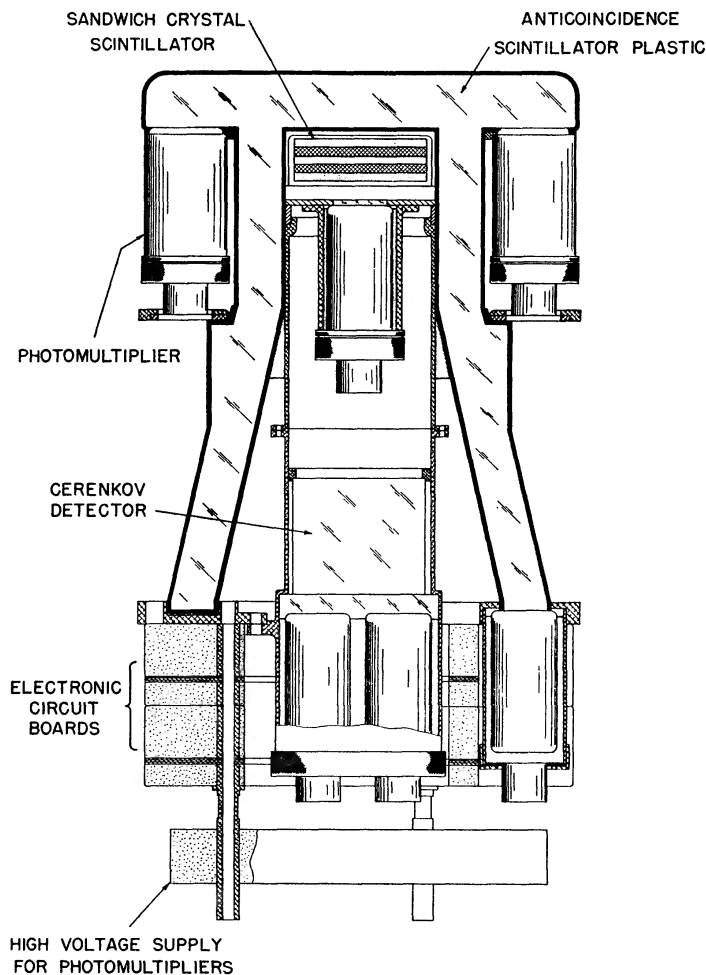


FIG. 2.—Schematic drawing of the gamma-ray detector

(1958). This spectrum has been folded with our measured efficiency and angular sensitivity functions to yield an effective solid-angle-area factor of  $1.0 \pm 0.3$  cm<sup>2</sup> sterad for the detector in the presence of an isotropic cosmic-ray-produced gamma-ray flux. The large uncertainty is the result of the poor statistical accuracy of the measured efficiency of the instrument at large angles.

The entire telemetry system as well as the satellite itself with the exception of the

glass Cerenkov counter. The Cerenkov counter served to calibrate the beam and so permit an absolute measurement of the detector efficiency with only a small correction for the non-uniformity of the gamma-ray beam profile.

We greatly appreciate the generous help of Drs R. L. Walker, H. Colbrak, J. Van Pulten and J. Mullins, all of C.I.T., in making these measurements.

gamma-ray detector was designed and constructed by the Marshall Space Flight Center (MSFC) of NASA. The satellite (Explorer XI or 1961 nu) was launched April 27, 1961, by a Juno II rocket into a 300–1100-mile  $28.8^\circ$  inclination orbit. The data were acquired by the Minitrack stations of NASA, by the MSFC Green Mountain tracking station, and by the South Point Hawaii station of the Pacific Missile Command. Magnetic tapes were forwarded from the stations to the Goddard Space Flight Center where the data were transferred via a multichannel oscilloscope to photographic film. The film data were reduced here at M.I.T. and analyzed with the aid of the M.I.T. Computation Center's IBM computers. With the exception of the pulse-height telemetry loss mentioned

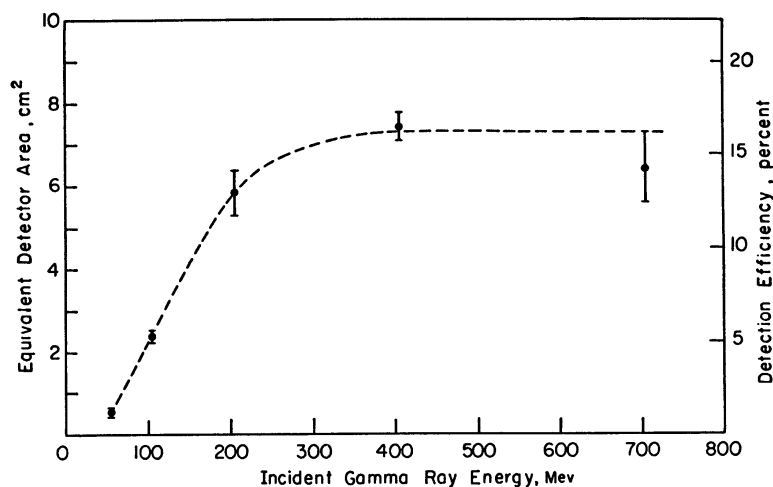


FIG. 3.—Detection efficiency in the forward direction

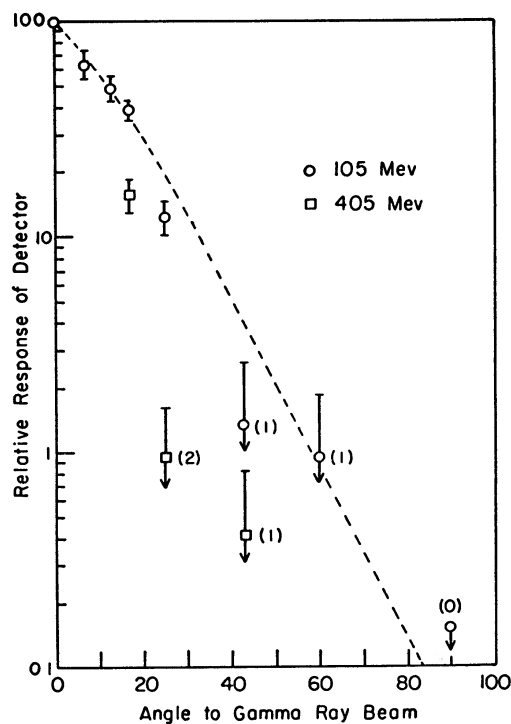


FIG. 4.—Angular response as measured at two gamma-ray energies

previously, and the tape-recorder failure, performance and stability in orbit were satisfactory for the first 2 months. A failure or deterioration of some portion of the primary power supply system required our discarding varying portions of the data for 5 additional months. About 7 months from launch the radio transmitter was turned off by radio command since the supply voltages were by then practically always below usable levels.

### III. SATELLITE MOTION AND ASPECT DETERMINATION

During launch the satellite was spin-stabilized and spun about its long axis at about 5 revolutions per second. This spinning mode persisted for about 2 weeks, somewhat longer than anticipated. During this period small magnetic torques precessed and decreased somewhat the angular momentum. Starting May 16, the cone of motion opened rapidly, and by May 19 the satellite had for all practical purposes reached its ultimate and stable motion of an end-over-end tumble about the transverse principal axis having the largest moment of inertia. The tumble period was initially 12 seconds and over the 7-month period increased to about 15 seconds. The angular momentum during this period precessed about 10 degrees a day, and it was this precession which permitted the gamma-ray detector to scan not just a plane but the entire celestial sphere.

The analysis of gamma-ray arrival directions required a knowledge of not only the plane of tumble (i.e., the angular momentum direction) but also of the instantaneous orientation of the satellite *in* this plane. Photoelectric devices sensitive to the Sun and to the reflected light from the Earth were included on the satellite and their outputs were telemetered to aid in aspect determination. But the most useful information came from the instantaneous radio power levels recorded during reception at the receiving stations. The transmitting antenna was the satellite structure itself, and it had nulls in its radiation pattern fore and aft, and in a cone at  $74^\circ$  to the forward direction. As the satellite traveled across the sky in range of a receiving station, the received radio power varied through a series of repeating nulls, minima and maxima that were characteristic of the orientation of the plane of tumble. The procedure for using this data was developed by personnel at MSFC (Nauman, Fields, and Holland 1962) and requires very accurate orbital data. Because the plane of tumble precessed relatively slowly, data taken by MSFC staff members at their Green Mountain station at Huntsville, Alabama, were sufficient to permit their determining the angular momentum directions from these data alone, and these determinations were kindly supplied to us. In the final analysis, however, we were forced to use the received radio power levels from all stations, because the tumble frequency changed irregularly and so much that even a quadratic fit to the tumble frequency versus time over 1 day led to unacceptable errors in the phase or instantaneous orientation. This unanticipated complication was probably the single most annoying and time-consuming part of the data reduction.

In general, satellite look-directions were determined to within about  $4^\circ$ , but we recognize that a few scattered determinations may be off by as much as  $15^\circ$ . In Figure 5 is shown the path of the celestial coordinates of the angular momentum and in Figure 6 is shown the tumble frequency (actually the constant term in one-day quadratic fits) as a function of time.

### IV. RESULTS

Of the total of about 7 months that the instrument was turned on and working in orbit, only 141 hours, or 3 per cent, have been culled as useful observing time. The fraction is small because the satellite was within range of a receiving station only 20 per cent of the time, was below the radiation belts only 30 per cent of the time, and had subnormal voltages for appreciable fractions of the fifth, sixth, and seventh months.

#### a) *Pulse-Height Data*

During these 141 hours, 1012 events were accepted as gamma rays by the circuit logic. As explained in Section II, information concerning the energy loss in the sandwich

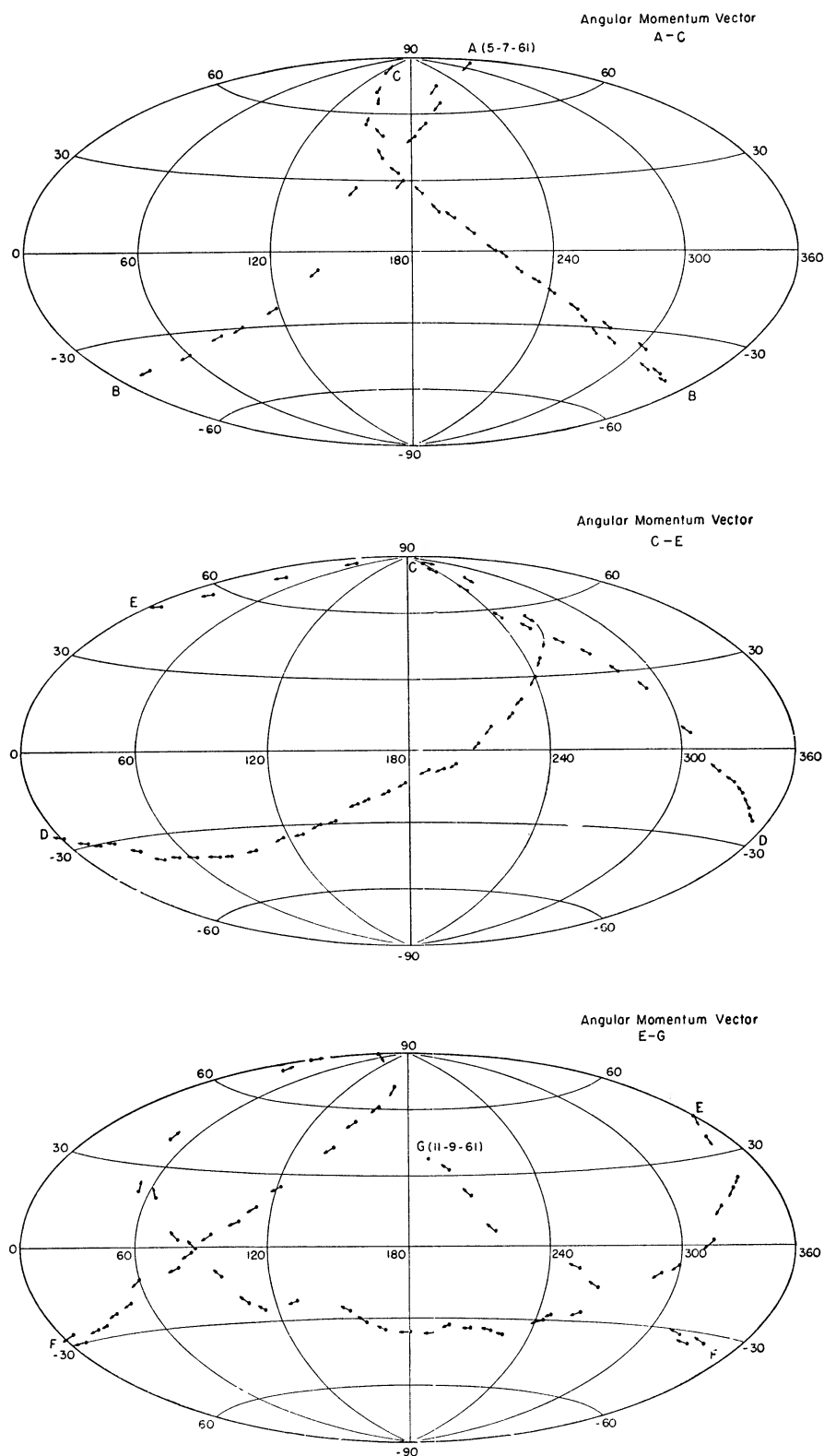


FIG. 5.—Path of the angular momentum vector of the satellite

scintillator was telemetered following each detected event. The pulse-height distribution for the 1012 events is shown in Figure 7. Also shown in Figure 7 is a sample pulse-height distribution for those events telemetered during the calibration periods when the veto counter was turned off. Notice that this later distribution is markedly different than the first in that there are relatively many more large pulses. In particular 11 per cent were so large that the telemetry circuits were saturated. With the veto counter turned off, the detector could respond to cosmic-ray protons, alpha particles, etc. In traversing the  $10 \text{ g cm}^{-2}$  sandwich detector there is about a 10 per cent chance that these particles will undergo a nuclear interaction, and it is to these interactions and incident heavy nuclei

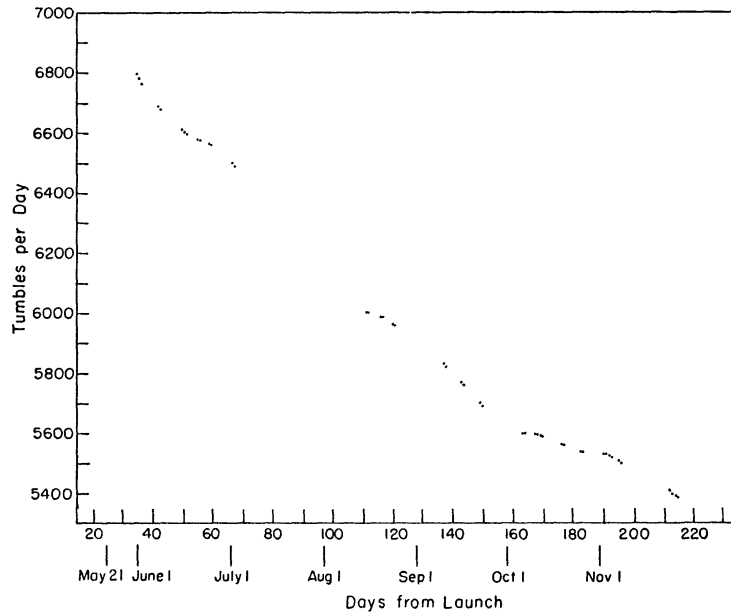


FIG. 6.—Tumble frequency during the satellite's useful life

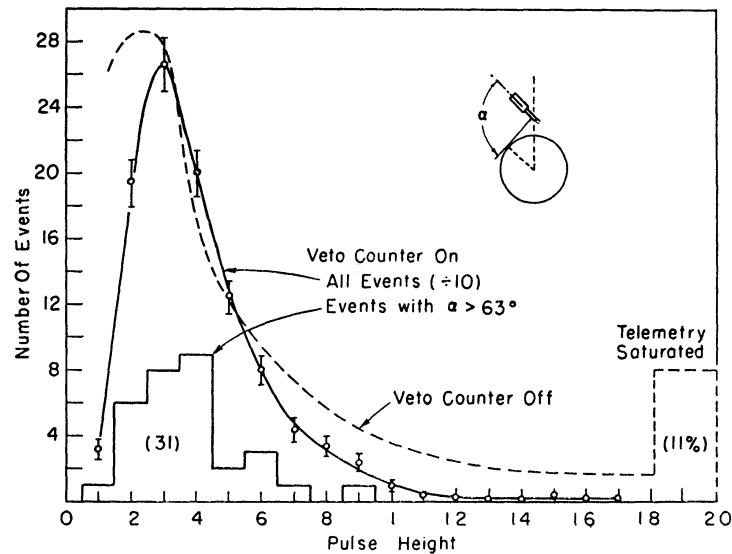


FIG. 7.—Distribution of pulse heights as measured in the sandwich detector

that we attribute the very large energy losses. No very large energy losses occurred when the veto counter was turned on. We regard this as good evidence that few, if any, of these events were caused by neutron interactions or veto counter inefficiency.

#### *b) Exposure-Time Evaluation*

The scan of the gamma-ray instrument about the sky was uncontrolled but by no means random. Hence, in order to evaluate apparent gamma-ray *intensities* from different parts of the sky, it was necessary to account carefully for the total amount of time the instrument was exposed to various directions.

In our first method of analysis and the one upon which our earlier reported results were based, this accounting was done in a rather literal sense. Eighty-two equal-area symmetrical cells were positioned as uniformly as possible in the sky. As the sensitive cone of the instrument swept across the sky in a single tumble, those cells near to the tumble plane were apportioned exposure time provided they were above a predetermined artificial horizon. During a single pass over a receiving station some cells were exposed each tumble. Others "set" below or "rose" above the artificial horizon. Others were not exposed at all. The amount of exposure a given cell received from a single tumble depended upon how far its center was from the tumble plane and on the tumble period. In all there were about 6000 useful passes (parts or all of many passes had to be excluded because the satellite was often above the lower boundary of the radiation belt) and about 250000 tumbles. The cumulative exposure time for any particular cell represented, therefore, the superposition of a very large number of short-duration exposures. Needless to say, this and other parts of the data analysis were feasible only with fast electronic computers.

We have recently developed an alternative and much more flexible analysis procedure. For each detected event we compute and store a rather large number of pertinent quantities. These include: Julian time to 0.1 sec, geographic and geomagnetic coordinates of the satellite, satellite orientation in celestial and galactic coordinates, the angle  $\theta$  between satellite axis and a line to the center of the Earth, the angle  $\alpha$  between the satellite axis and the horizon, the angle  $\beta$  between the satellite axis and a line to the Sun, etc. During the period of each useful pass over a receiving station, random events have been generated at a rate such that their total number is about 25 times the total number of real events. (The actual rate corresponded to one every 20.4 sec, and the events were randomly spaced so as to avoid any possible lock-in phenomena with the satellite tumble period). These random events were treated in the same way as the detected events in all respects. To evaluate an intensity one merely sorts both sets of events according to the same criteria (e.g., all events for which the galactic latitude was less than  $10^\circ$  which occurred while the satellite was between  $30^\circ$  and  $35^\circ$  geomagnetic latitude) and regards each random event as being worth 20.4 sec of exposure time. There is a statistical uncertainty associated with this method of exposure time evaluation, but with 25 times as many random as detected events, the uncertainty is negligible compared to that arising from the much smaller number of detected events. Both methods of analysis have been used on some portions of the data, and in all cases where comparisons could be made the agreement has been excellent. Much of the analysis discussed in the following paragraphs was only practical with the second, or Monte Carlo, method.

#### *c) Distribution Relative to the Earth*

Many gamma rays are produced by cosmic rays in their collisions with the atmosphere of the Earth. Hence the Earth should appear bright in gamma rays against the very weak intensity expected from space.

Gamma rays from the Earth are discussed best with directions referred to a satellite-centered coordinate system, the polar angle being measured from the direction to the center of the Earth. In this coordinate system the horizon is at a polar angle  $\theta = h \approx 64^\circ$ ,

which varied somewhat because the satellite height above the Earth varied between the extremes of its 300-mile perigee and 1100-mile apogee. The zenith corresponds, of course, to  $\theta = 180^\circ$ . In Figures 8 and 9 is shown the relative intensity (actually the ratio of detected to random events or events per 20.4 sec) plotted versus  $\cos \theta$ . Evidently, and as is to be expected, the horizon of the Earth emits many gamma rays. This limb brightening was detected in the balloon-borne emulsion experiment of Svenson (1958). While the apparent intensity drops off rapidly just beyond the horizon, there remains evidence of a tail or residual intensity associated with the Earth out to rather large angles ( $\cos \theta \approx -0.6$ ). This tail is clear evidence that our data taken when  $\theta < 127^\circ$  ( $\alpha < 63^\circ$  above

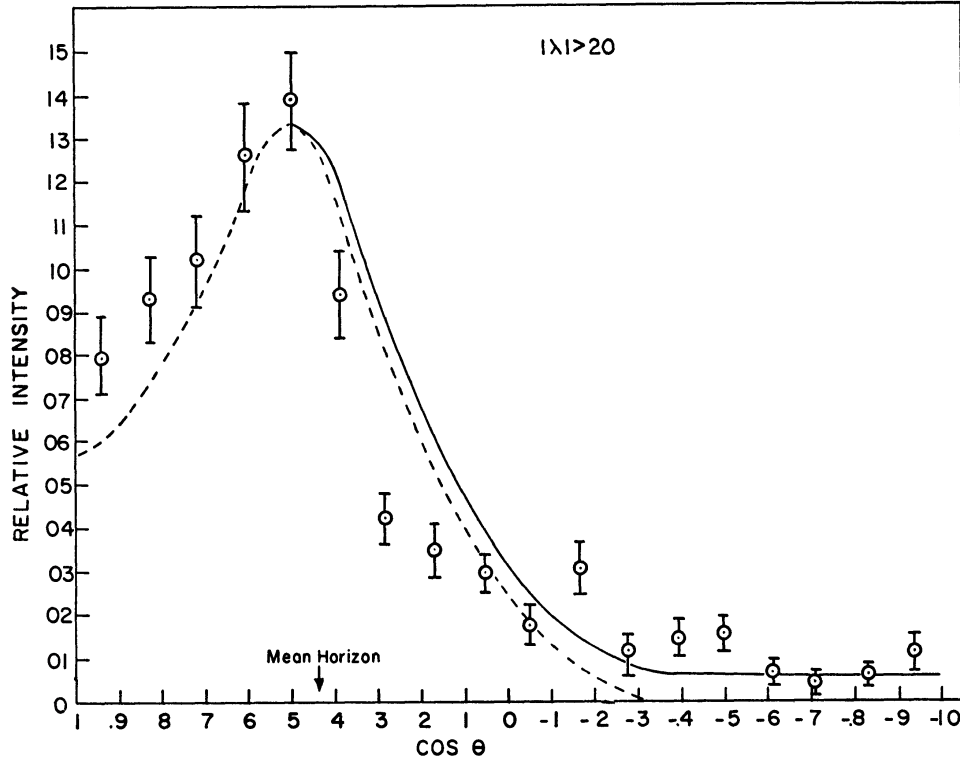


FIG. 8.—Distribution of gamma-ray arrival directions relative to the Earth. The center of the Earth corresponds to  $\theta=0^\circ$ , and the zenith is at  $\theta=180^\circ$ . The data shown above were taken while the satellite was more than  $20^\circ$  from the geomagnetic equator.

the horizon) certainly contain a contaminating component somehow associated with the presence of the Earth. From this data alone it is not possible to exclude the possibility that the data taken when  $\theta > 127^\circ$  is partially or even totally background that is related to the Earth and its albedo. The relative extraterrestrial gamma-ray intensity which should be regarded as an upper limit, based only on data taken when  $\theta > 127^\circ$ , corresponds to .0067 events/random event or  $3.3 \times 10^{-4} \text{ sec}^{-1}$ . Since the solid-angle-area-efficiency factor was measured to be  $1.0 \pm 0.3$ , the upper limit to the extraterrestrial intensity in absolute units is

$$I = (3.3 \pm 1.2) \times 10^{-4} \text{ cm}^2 \text{ sec}^{-1} \text{ sterad}^{-1}. \quad (1)$$

The total number of measured events that contributed to the above estimate was 31. The large quoted error arises primarily from the uncertainty in the solid-angle-area-efficiency factor.

d) *Effect of Geomagnetic Latitude*

As the satellite orbited the Earth in its inclined orbit, it covered a region of geomagnetic latitude in the range  $\lambda = -42^\circ$  to  $42^\circ$ . Since there is appreciable variation of the incident cosmic-ray intensity with geomagnetic latitude, one would expect similar variations in the intensity of albedo gamma rays. A comparison of Figures 8 and 9 shows that this is indeed the case. On Figure 8 is shown data accumulated while the satellite was more than  $20^\circ$  from the geomagnetic equator, while for Figure 9 the satellite was within  $20^\circ$  of the geomagnetic equator. Figure 10, where intensity has been plotted versus geomagnetic latitude, shows the effect more clearly. The upper set of points are for gamma rays which arrived from the direction of the Earth, center to true horizon. The lower set of points are for gamma rays which arrived at least  $63^\circ$  above the Earth's horizon. There

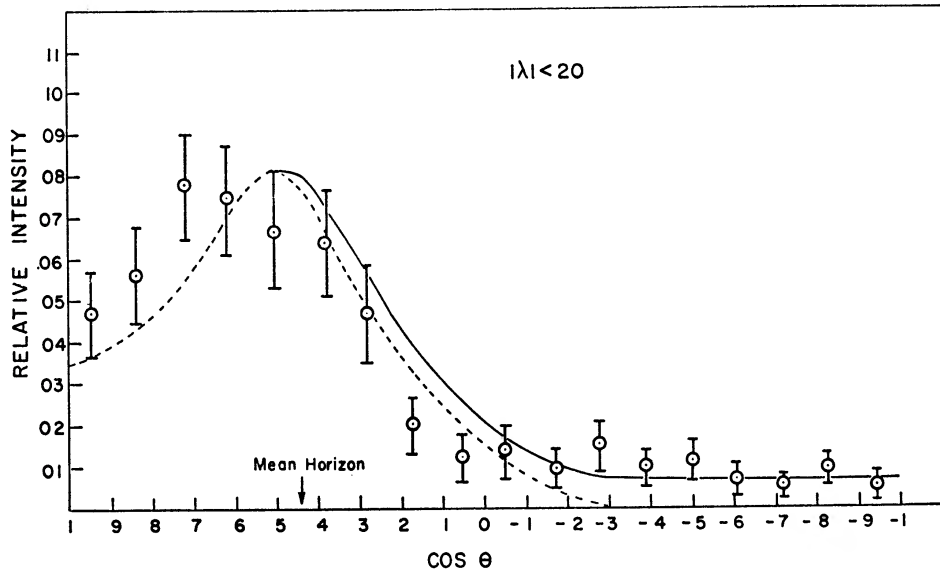


FIG. 9.—Distribution of gamma-ray arrival directions relative to the Earth. The data shown above were taken while the satellite was within  $20^\circ$  of the geomagnetic equator.

should, of course, be no geomagnetic latitude effect for gamma rays of extraterrestrial origin, and while the data points appear to lie along a single horizontal line they are probably also consistent in a statistical sense with a hypothetical variation similar to that indicated by the upper set of points. It is of interest to consider the ratios of the relative intensities for two bands of geomagnetic latitude, one for which  $|\lambda| > 20^\circ$ , the other for which  $|\lambda| < 20^\circ$ . For the albedo gamma rays this ratio is

$$\frac{I(|\lambda| > 20^\circ)}{I(|\lambda| < 20^\circ)_{\text{albedo}}} = 1.65 \pm 0.16, \quad (2)$$

while for the gamma rays from near the zenith, the corresponding ratio is

$$\frac{I(|\lambda| > 20^\circ)}{I(|\lambda| < 20^\circ)_{\text{zenith}}} = 1.16 \pm 0.44. \quad (3)$$

Had this result more statistical significance, the evidence would be very strong that those gamma rays from near the zenith were indeed of extraterrestrial origin. As it is, we can only say that the evidence does not favor their being of terrestrial origin.

*e) Intensity and Distribution of Albedo Gamma Rays*

The angular resolution of the detector is very broad, and it is clear that only the very coarse features of the albedo gamma-ray distribution can be resolved. We find, in fact, that a fairly good fit to our data can be obtained if one assumes that the Earth, as viewed in gamma rays at the height of the satellite, emits more or less uniformly and isotropically over the disk (*a* of Fig. 11) except for a bright band at the horizon (*b* of Fig. 11). When these distributions are folded with the approximate measured angular response of the detector, there result the curves labeled *a'* and *b'*. In this folding process, the angular response of the instrument was approximated by

$$F(a) = 2[1 + \exp(a/11)]^{-1}, \quad (4)$$

where  $F(a)$  is the relative response of the detector to a gamma-ray beam at an angle  $a$  (in degrees) off-axis. (The dashed line on Fig. 4 is  $F(a)$ .) The relative amounts of the  $a$  and  $b$  components may be added (curve marked *Sum*) to give a reasonable fit to the experimental data.

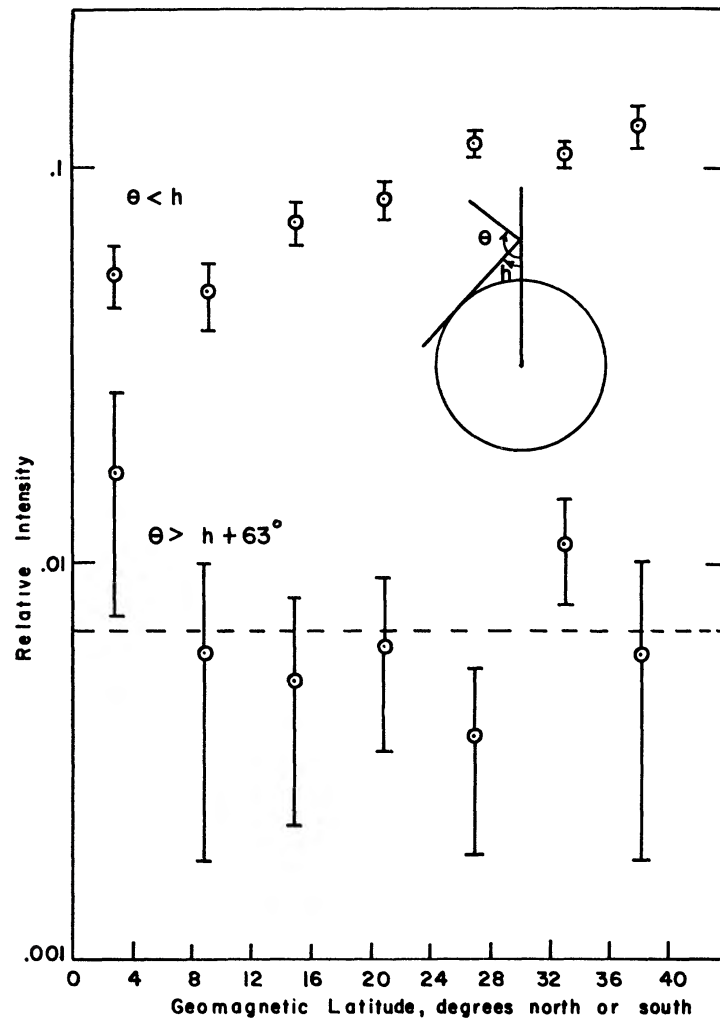


FIG. 10.—Intensity of gamma rays from the Earth (upper set of data points) and from the sky (lower set of data points) as functions of the geomagnetic latitude of the satellite.

Under the assumptions outlined above, the omnidirectional intensity at the height of the satellite is

$$J = \Omega_E I_E + F/\cos h + (4\pi - \Omega_E)I, \quad (5)$$

where  $\Omega_E = 2\pi(1 - \cos h)$  is the solid angle of the Earth's disk,  $I_E$  is the albedo intensity of the Earth,  $F/\cos h$  is the flux from the horizon which is at polar angle  $\theta = h$  ( $F$  is the outgoing component of this flux), and  $I$  is the intensity from the sky.  $J$  is obtained from our data,  $I$  is taken to be the upper limit discussed previously,  $\Omega_E$  and  $h$  are 3.51 steradians and  $64^\circ$  at a typical height of the satellite (710 km) and  $(F/\cos h)/(\Omega_E I_E) = 1.92$  has been chosen to make the *Sum* curve of Figure 11 conform to the data.  $J$ ,  $I_E$ , and  $F$  have been computed for both geomagnetic latitude bands and are summarized in Table 1. There is an uncertainty of about 30 per cent associated with each of the tabulated quantities, and this has arisen from the uncertainty in the solid-angle-area-efficiency

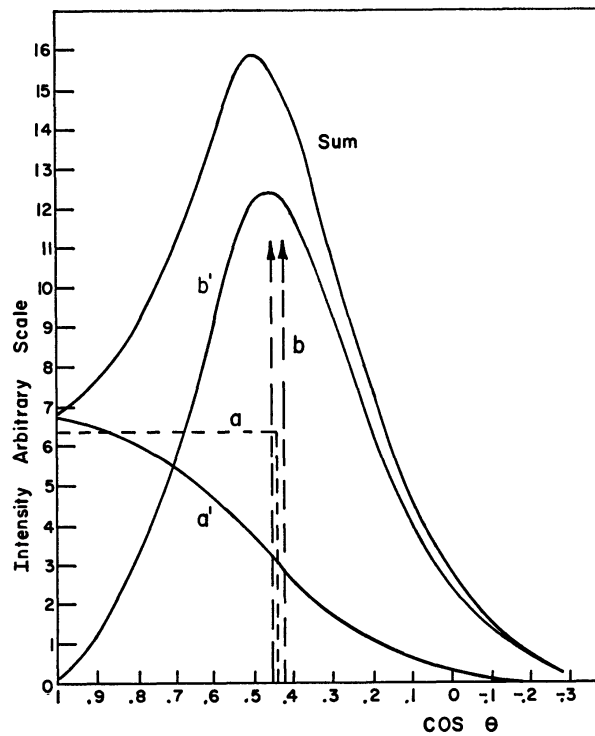


FIG. 11 —The measured distribution of gamma rays from the Earth can be explained reasonably well by assuming a uniformly bright disk and a bright band of negligible angular width at the horizon.

TABLE 1  
OMNIDIRECTIONAL AND ALBEDO INTENSITY AT 710-KM ALTITUDE  
FOR TWO BANDS OF GEOMAGNETIC LATITUDE

	$J(\text{cm}^{-2} \text{sec}^{-1})$	$I_E(\text{cm}^{-2} \text{sec}^{-1} \text{sterad}^{-1})$	$F(\text{cm}^{-2} \text{sec}^{-1})$
$20^\circ <  \lambda  < 42^\circ$	$2.8 \times 10^{-2}$	$2.5 \times 10^{-3}$	$7.3 \times 10^{-3}$
$ \lambda  < 20^\circ$	$1.9 \times 10^{-2}$	$1.5 \times 10^{-3}$	$4.6 \times 10^{-3}$

factor. The broken curves of Figures 8 and 9 have been calculated under the assumptions outlined above but with  $I$  taken to be zero. The solid curves show the effect of including a sky intensity equal to our measured value.

$I_E$  should not vary with height above the atmosphere, while  $F$  should vary as the inverse square of distance to the Earth's center. The contribution of  $F$  to  $J$ , on the other hand, varies as  $(R^2 \cos h)^{-1}$  and becomes very large at altitudes just above the Earth's atmosphere. Great caution must therefore be exercised in attempts to infer an extraterrestrial gamma-ray intensity from measurements made with a vertical-pointing detector near the top of the atmosphere. Practical detectors are bound to have some response to horizontally moving gamma rays, and it is to this apparent intensity that measurements plotted versus atmosphere depth will extrapolate, even if the extraterrestrial intensity is immeasurably small.

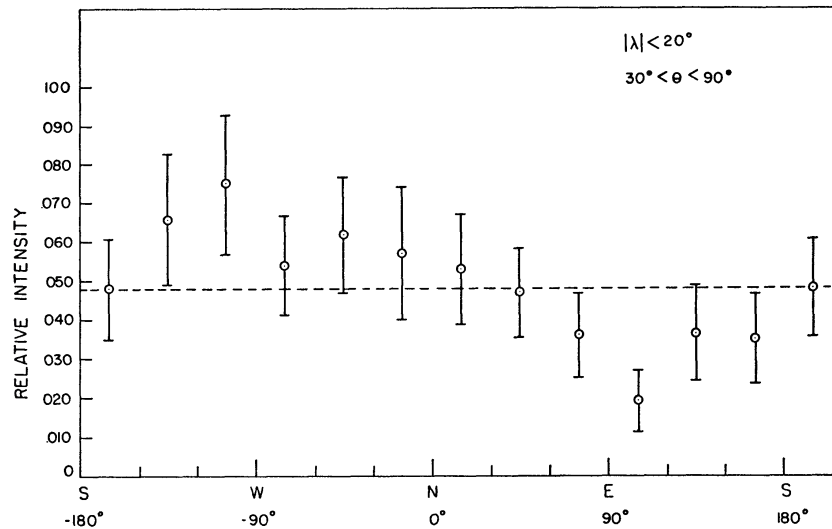


FIG. 12.—Azimuthal dependence of gamma rays from near the Earth's horizon

#### f) East-West Effect

The limb brightening mentioned previously is clear evidence that cosmic rays which strike the atmosphere at glancing incidence may produce gamma rays with not very large change in direction and presumably through  $\pi^0$  meson production and decay. Near the top of the atmosphere and particularly at the geomagnetic equator the intensity of primary cosmic rays is markedly dependent upon arrival direction in the local N.S.-E.W. plane. Protons arriving from the east and west must have momenta of at least 60 and 10 BeV/c, respectively. Gamma rays from the Earth's horizons as detected by a satellite should therefore be more intense from the west horizon than from the east. Our data taken near the geomagnetic equator (see Fig. 12) show this effect, although with but poor statistical significance.

Several effects tend to diminish what would otherwise be expected to be a large asymmetry. Most important is the fact that the detector solid angle subtends not just the horizon but a large portion of the Earth's disk as well. Albedo from the Earth's disk must involve gamma rays that carry but little history of the primary particle's direction. We estimate that  $\frac{1}{3}$  of the apparent intensity from the west is in fact from the disk. The large solid angle has the additional tempering effect of including not only a range of azimuthal directions but also of including portions of the horizons at geomagnetic latitudes far from that of the satellite itself.

g) *Celestial Distribution*

The total number of events which arrived more than  $\alpha = 63^\circ$  above the Earth's horizons was only 31. With so small a statistical sample only a very pronounced celestial anisotropy would reveal itself. Nevertheless, the data have been examined carefully, particularly for any indication of concentration toward the galactic plane or toward any of the strong radio sources. The result of this analysis is rather clear. The observed celestial distribution is consistent with isotropy.

In Figure 13 is shown the observed intensity plotted versus galactic latitude. Data taken at equivalent positive and negative latitudes have been combined in making this

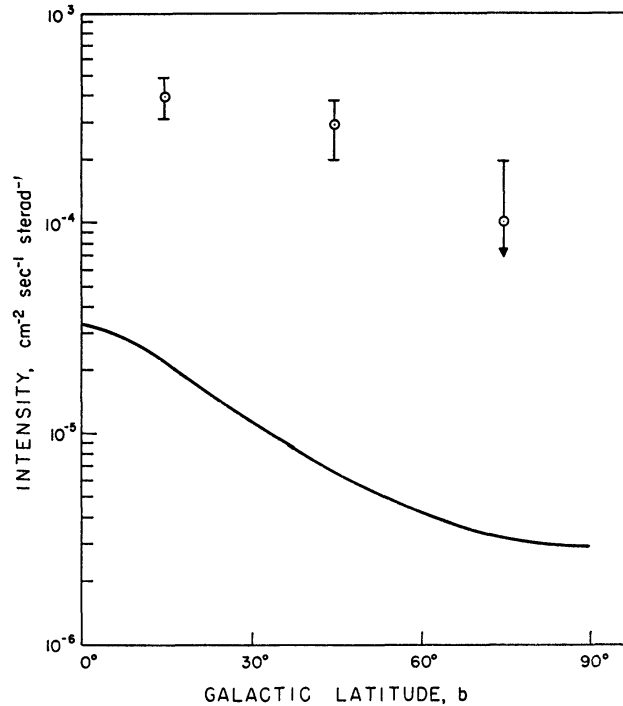


FIG. 13.—Observed intensity as a function of galactic latitude. The smooth curve is the predicted intensity from the  $\pi^0$ -decay process. It is based upon the observed galactic atomic hydrogen and the assumption that the cosmic-ray intensity as measured near the Earth is the same throughout the Galaxy.

plot. While the intensity seems to drop off with increasing latitude, the tendency is not statistically significant. The ratio of the average intensity within  $45^\circ$  of the galactic plane to the average intensity within  $45^\circ$  of the galactic poles is

$$\frac{I(|b| < 45^\circ)}{I(|b| > 45^\circ)} = 1.6 \pm 0.6. \quad (6)$$

If the gamma-ray intensity were strictly proportional to the number of hydrogen atoms per  $\text{cm}^2$  integrated along the line of sight, this ratio would be 3.7.

Approximate upper limits to the intensity from a number of celestial objects are given in Table 2. These upper limits were evaluated as follows. The number of detected events and number of random events which occurred while the instrument pointed within an angle  $\theta_0 = 17^\circ$  (solid angle  $\Omega_0 = 2\pi[1 - \cos \theta_0]$ ) centered on a radio source were tabulated. The number of random events provided a measure of the time  $T$  that the instrument axis pointed within  $\Omega_0$ . It was assumed that directions within  $\Omega_0$  were scanned uniformly and

that the supposed gamma-ray flux  $F(E)$  had an energy spectrum such that  $F(E) = F_0 f(E)$  where  $f(E)$  is a normalized  $\pi^0$ -decay spectrum. Actually,  $f(E)$  was taken to be the same emulsion-measured spectrum that was used in the detector efficiency computation discussed in Section II. If  $K(E, \theta)$  represents the response of the detector—the probability that a gamma ray of energy  $E$  incident at an angle  $\theta$  off-axis is detected—the expected number of detected events is

$$N = \frac{ATF_0}{\omega_0} \int_0^\infty f(E) dE \int_0^{\theta_0} 2\pi \sin \theta K(E, \theta) d\theta. \quad (7)$$

Our calibration data have permitted the integrals to be evaluated to within about 30 per cent, and this uncertainty must, of course, be associated with values of  $F_0$ . In assigning the upper limits, we have taken the number of events,  $N$ , to be one more than the number actually detected. Needless to say, the fact that some of the values of  $F_0$  listed in Table 2 are larger than others simply reflects the non-uniform nature of the sky exposure. In no case is the existence of a finite measured flux claimed.

TABLE 2  
DATA AND APPROXIMATE GAMMA-RAY FLUX UPPER LIMITS FOR A  
NUMBER OF POSSIBLE DISCRETE SOURCES

Source	Detected Events	Random Events	Flux Upper Limit
Andromeda . . . . .	0	17	16 $\times 10^{-4} \text{cm}^{-2} \text{sec}^{-1}$
Small Magellanic Cloud	0	25	11
Large Magellanic Cloud	0	29	9 4
Taurus A . . . . .	2	123	6 6
Hydra A . . . . .	0	155	1 7
Virgo A . . . . .	1	199	2 7
Centaurus A	0	90	3
Hercules A . . . . .	1	156	3 4
Cygnus A . . . . .	1	107	5
Cassiopeia A	1	23	23
Galactic center	2	154	5 3

#### *h) Solar Flares*

Quite by accident, the tumble plane of the satellite passed near the Sun during two rather large solar flares. The first, that of July 12, 1961, was of class 3 and the tumble plane was  $3^\circ$  from the Sun. The flare maximum was about 10:20 GMT and the visual evidence ceased at 13:00. Our observations covered a  $2\frac{1}{4}$ -min period starting at 11:25. No gamma rays were detected, and we infer that the average flux from the Sun during this period was not larger than  $10^{-2} (\text{cm}^2 \text{sec})^{-1}$ .

The second, that of July 18, 1961, was of class 3+ and the tumble plane was  $32^\circ$  from the Sun. The flare maximum was at about 09:30 GMT and visual evidence ceased at 12:10. Our observation covered an 8-min period starting at 09:29. Again no gamma rays were detected, and we infer that the average flux from the Sun during this period was not larger than  $1.5 \times 10^{-2} (\text{cm}^2 \text{sec})^{-1}$ .

#### *i) Comparison with Other Experiments*

The balloon-borne experiment of Duthie, Hafner, and Kaplon (1963) in which the counting rate of gamma rays was extrapolated to zero thickness of atmosphere gives an apparent intensity of  $(5.4 \pm 0.7) \times 10^{-3} \text{cm}^{-2} \text{sec}^{-1} \text{sterad}^{-1}$ . This intensity is more than a factor of 10 larger than ours, although we understand that in more recent experiments

a lower intensity has been measured. As explained in Section III*e*, we feel that the large horizon albedo makes an extrapolation procedure hazardous. We see no evidence in our data of the sidereal time variation or celestial anisotropy reported by Hafner, Duthie, Kaplon, and Fazio (1963).

Cline (1961) has also carried out a balloon experiment in which the counting rate of gamma rays was extrapolated to zero thickness of atmosphere. Collimation in Cline's case depended upon a very thick lead shield, and the response to a horizontally moving flux was very small. His extrapolated intensity was  $(1 \pm 3) \times 10^{-3} \text{ cm}^{-2} \text{ sec}^{-1} \text{ sterad}^{-1}$ , entirely consistent with ours.

## V. DISCUSSION

It was mentioned in Section IV that the measured gamma-ray intensity is not consistent with that one would expect from cosmic-ray collisions with interstellar atomic hydrogen. The expected directional intensity of gamma rays from this source has been estimated as follows.

Let  $S = n q$  be the number of  $\pi^0$ -decay gamma rays which are produced per ( $\text{cm}^3 \text{ sec sterad}$ ) in a region in which there are  $n$  hydrogen atoms per  $\text{cm}^3$ . The quantity  $q$  depends only on meson production cross-sections and the assumed cosmic-ray flux. If the cosmic-ray flux is taken to be the same as it is near the Earth,  $q$  as given by Pollack and Fazio (1963) is  $9.7 \times 10^{-27} (\text{sec sterad})^{-1}$ . The directional intensity of these gamma rays is then

$$I' = q \int_0^r n d\mathbf{r} = q N_H \quad (8)$$

where the integral is carried out along the line of sight and out to whatever  $r$  is appropriate, e.g., the edge of the Galaxy.  $N_H$  can be obtained more or less directly from radio astronomical 21-cm measurements. Erickson, Helfer, and Tatel (1959) have in fact published a map which shows contours of constant  $N_H$ . We have extended this map using the line profiles of Muller and Westerhout (1957) and for the directions accessible only from the southern hemisphere, the profiles taken by the Sydney group (McGee, Murray, and Milton 1963; McGee and Milton 1964). (In those directions in which the optical depth was large, we have assumed a spin temperature of  $125^\circ \text{ K}$ .)  $I'$ , as defined above, cannot be compared with measured intensities because in general it is not constant over the sensitive solid angle of practical gamma-ray detectors. We have therefore computed appropriate average values of  $\bar{N}_H$  defined as

$$\bar{N}_H(b, l) = \int N_H(b, l) g(\alpha) d\Omega, \quad (9)$$

where  $N_H(b, l)$  is the number of hydrogen atoms  $\text{cm}^{-2}$  along the line of sight defined by  $b$  and  $l$ , and  $g(\alpha)$  is the normalized angular response function of the detector. The predicted gamma-ray intensity as measured by the instrument is then simply  $I = q \bar{N}_H$ . We have averaged  $I$  over galactic longitude, and the resulting dependence of  $I$  upon galactic latitude is the solid curve shown in Figure 13.

Our measured upper limits are some 10–20 times as large as the values indicated by the curve. The angular dependence, because of the statistical uncertainty, is essentially consistent with both isotropy and the curve. While we do not wish to detract from the impression that some or conceivably all of our measured intensity could in fact be background, we wish to discuss briefly several alternative possibilities that may be more attractive from an experimentalist's point of view.

### *a) Interstellar Molecular Hydrogen*

Gould and Salpeter (1963) and Gould, Gold, and Salpeter (1963) have recently considered the formation and dissociation mechanisms and the likely galactic distribution

of molecular hydrogen. They suggest that molecular and atomic hydrogen are, on the average, similarly distributed and that the relative abundance may be in the range 0.1 to 10. Thus molecular hydrogen, if present with a concentration near the larger values suggested by the above authors, could account for the high intensity.

*b) Galactic Cosmic-Ray Intensity*

Parker (1958) has suggested that the cosmic-ray intensity in the Galaxy as a whole may be appreciably larger than it is near the Earth as a result of the interaction of galactic cosmic rays with the moving magnetic field carried by the solar wind. If this mechanism is operative, it is certain that the energy spectrum as well as the cosmic-ray intensity would be altered. The net effect on the gamma-ray intensity is difficult to estimate.

While these two mechanisms (*a*) or (*b*) could help account for our large gamma-ray intensity, they would also serve to inject more electron energy into interstellar space via charged meson decay than is ordinarily assumed. This in itself would not be in conflict with the total galactic continuum noise power (Ginzburg and Syrovatsky 1963) especially if leakage from the Galaxy is an important cause of electron loss (Burbidge and Gould 1963). On the other hand, the recent observations of De Shong, Hildebrand, and Meyer (1964), which show that there are more electrons than positrons in the primary electron component, indicate that some appreciable fraction of the radio noise is made by directly accelerated, not collision-produced, electrons.

*c) Intergalactic Cosmic Rays*

It is possible that cosmic rays are a universal phenomena with an intensity everywhere, including intergalactic space, about the same as that found locally. Intergalactic cosmic rays could then produce  $\pi$  mesons in collisions with whatever intergalactic gas there may be. The gamma-ray intensity from this source would then be  $I = nRq$ , where  $n$  is the intergalactic gas density and  $R$  is a distance of the order of, but less than, the Hubble radius. We shall take  $R$  to be  $6 \times 10^{28}$  cm. The gas density is unknown. The only firm information is the upper limit to the intergalactic atomic hydrogen density, about  $10^{-5}$  cm $^{-3}$  (Field 1962; Goldstein 1963). This upper limit is near the "cosmological" value preferred in some cosmologies, but is about 30 times as large as the smoothed-out density of all observable matter in galaxies. With  $10^{-5}$  cm $^{-3}$  for the density we have  $I \approx 6 \times 10^{-4}$  (cm $^2$  sec sterad) $^{-1}$ , comparable with our upper limit.

*d) Intergalactic Electrons*

Felten and Morrison (1963) have suggested that the apparent isotropic component of cosmic X-rays (Giacconi, Gursky, Paolini, and Rossi 1962), low-energy gamma rays (Arnold, Metzger, Anderson, and Van Della 1962), and gamma rays of  $\approx 100$  MeV under discussion here may have a common origin in the inverse Compton collisions of possible intergalactic electrons with the photons of starlight. The following considerations are in no essential way different from those of Felten and Morrison, but the argument is tailored for the present context. Gamma rays in the  $W = 100$  MeV region may be produced in Compton collisions between photons of energy  $\epsilon \approx 3$  eV and electrons of energy

$$E \approx m c^2 \sqrt{\frac{W}{\epsilon}}. \quad (10)$$

The cross-section for the process in this energy region is just the Thompson cross-section,  $\sigma = (8\pi/3)r_e^2$ . If  $I_e$  is the directional intensity of intergalactic electrons of energy greater than  $E$ , the directional intensity of gamma rays of energy greater than  $W$  is

$$I = I_e \sigma \frac{\rho}{\epsilon} R \quad (11)$$

where  $\rho$  is the energy density of (optical) photons,  $R$  is as discussed under Section Vc, and  $W$  and  $E$  are related according to equation (10).

The integral gamma-ray intensity to be inferred from our measurement depends somewhat upon the shape of the assumed energy spectrum. This is because the efficiency versus energy relationship (see Fig. 3) is not a step function. If we take the differential energy spectrum to be of the form  $W^{-\gamma}$  with  $\gamma = 1.7$ , the upper limit to the integral intensity of gamma rays of  $W > 100$  MeV is

$$I = 2 \times 10^{-4} (\text{cm}^2 \text{ sec sterad})^{-1}. \quad (12)$$

The intergalactic energy density of starlight,  $\rho$ , is known only very poorly. The question has been discussed by McVittie (1962), who shows how  $\rho$  for 1-eV photons depends upon the assumed cosmological model and value taken for the Hubble constant. We have integrated over photon energy and find that  $\rho \approx 2 \times 10^{-3} F^4$  eV/cm<sup>3</sup> where the Hubble constant is  $75F(\text{km sec}^{-1} \text{ mpc}^{-1})$ . The uncertainty in  $F$  obscures the dependency of  $\rho$  on reasonable cosmological models.

The upper limit to the intergalactic integral intensity of electrons of energy greater than 3 BeV is then

$$I_e < 7 \times 10^{-5} F^{-3} (\text{cm}^2 \text{ sec sterad})^{-1} \quad (13)$$

or, with  $F = 1$ , about 1 order of magnitude smaller than the corresponding integral intensity implied by the direct cosmic electron measurements of Earl (1961), Meyer and Vogt (1961), and Dilworth and Scarsi (1963). In other words, our result shows that the intergalactic electron intensity is at least a factor of 10 smaller than the intensity near the Earth. Felten and Morrison's factor is nearer 100, and the difference is due primarily to their different choice of a value for  $\rho$ .

Finally, as was discussed in our first report, the Explorer XI instrument was sensitive to gamma rays arriving from possible proton-antiproton annihilation processes. These give rise, through  $\pi^0$ -meson decay, to a gamma-ray spectrum sharply peaked about 70 MeV. At 70 MeV the solid-angle-area-efficiency factor of our instrument is about  $0.8 \text{ cm}^2 \text{ sterad}$  and the intensity of such gamma rays must be less than  $I = 4 \times 10^{-4} (\text{cm}^2 \text{ sec sterad})^{-1}$ . For a gas density in excess of  $10^{-3} \text{ cm}^{-3}$  the mean lifetime of antiprotons is less than the age of the Galaxy. Hence, adopting  $10^{-3} \text{ cm}^{-3}$  or more for the density of gas in the galactic halo, we may infer from our measurement an upper bound to the antiproton production rate in this region. This production rate is  $S = 4\pi I/mr$ , where  $I$  is the gamma-ray intensity mentioned above,  $m = 4$  is the approximate number of gamma rays per annihilation, and  $r = 2 \times 10^{22} \text{ cm}$  is the approximate average distance between the Earth and the edge of the halo. From this we have  $S < 10^{-25} (\text{cm}^3 \text{ sec})^{-1}$ . Cosmological models which require proton-antiproton creation at a rate as large as  $3 \times 10^{-22} (\text{cm}^3 \text{ sec})^{-1}$  seem therefore to be ruled out.

We are indebted particularly to Dr. James Kupperian of NASA's Goddard Space Flight Center. Dr. Kupperian skilfully and patiently co-ordinated the efforts of MSFC, GSFC, and M.I.T., through the design, construction, launch, and data-acquisition periods.

#### REFERENCES

- Arnold, J. R., Metzger, A. E., Anderson, E. C., and Van Dilla, M. A. 1962, *J. Geophys. Res.*, **67**, 4878.  
 Burbidge, G. R., and Gould, R. J. 1963, Proceedings of International Conference on Cosmic Rays, Jaipur.  
 Carlson, A. G., Hooper, J. E., and King, D. T. 1950, *Phil. Mag.*, **41**, 701.  
 Cline, T. J. 1961, *Phys. Rev. Letters*, **7**, 109.  
 De Shong, J. A., Jr., Hildebrand, R. H., and Meyer, P. 1964, *Phys. Rev. Letters*, **12**, 3.  
 Dilworth, C., and Scarsi, L. 1963, Proceedings of International Conference on Cosmic Rays, Jaipur.  
 Duthie, J. G., Hafner, E. M., Kaplon, M. F., and Fazio, G. G. 1963, *Phys. Rev. Letters*, **10**, 364.  
 Earl, J. A. 1961, *Phys. Rev. Letters*, **6**, 125.

- Erickson, W. C., Helfer, H. L., and Tatel, H. E. 1959, *Paris Symposium on Radio Astronomy* (Stanford, Calif.: Stanford University Press).
- Felten, J. E., and Morrison, P. 1963, *Phys. Rev. Letters*, **10**, 453
- Field, G. B. 1962, *Ap. J.*, **135**, 684.
- Garmire, G. 1963, *J. Geophys. Research*, **68**, 2627.
- Giacconi, R., Gursky, H., Paolini, F. R., and Rossi, B. B. 1962, *Phys. Rev. Letters*, **9**, 439
- Ginzburg, V. L., and Syrovatsky, S. T. 1963, Proceedings of International Conference on Cosmic Rays, Jaipur.
- Goldstein, S. J., Jr. 1963, *Ap. J.*, **138**, 978.
- Gould, R. J., Gold, T., and Salpeter, E. E. 1963, *Ap. J.*, **138**, 408
- Gould, R. J., and Salpeter, E. E. 1963, *Ap. J.*, **138**, 393
- Greisen, K. 1960, *Ann. Rev. Nuclear Sci.*, **10**, 63.
- Hafner, E. M., Duthie, J. G., Kaplon, M. F., and Fazio, G. G. 1963. Proceedings of International Conference on Cosmic Rays, Jaipur.
- Kraushaar, W. L. and Clark, G. W. 1962, *Phys. Rev. Letters*, **8**, 106
- McGee, R. X., and Milton, J. A. 1964, *Australian J. Phys.*, **17**, 128
- McGee, R. X., Murray, J. D., and Milton, J. A. 1963, *Australian J. Phys.*, **16**, 136.
- McVittie, G. C. 1962, *Phys. Rev.*, **128**, 2871.
- Meyer, P., and Vogt, R. 1961, *Phys. Rev. Letters*, **6**, 193.
- Morrison, P. 1958, *Nuovo Cimento*, **7**, 858.
- Muller, C. A., and Westerhout, G. 1957, *B.A.N.*, **13**, 151.
- Nauman, R. J., Fields, S. A., and Holland, R. L. 1962, *J. Geophys. Research*, **67**, 3619.
- Parker, E. N. 1958, *Phys. Rev.*, **110**, 1445.
- Pollack, J. B., and Fazio, G. G. 1963, *Phys. Rev.*, **131**, 2684.
- Savedoff, M. P. 1959, *Nuovo Cimento*, **13**, 12.
- Svennson, G. 1958, *Ark. Fys.*, **13**, 347.